Review

Overview of interfacial interaction mechanisms of bubble-mineral systems at the nanoscale

Zhoujie Wang[1,2], Yan Xiang[1,2], Jingyi Wang[3], Zhiyong Gao[2], Wei Sun[2], Lei Xie[1,2] iD

[1]State Key Laboratory of Complex Nonferrous Metal Resources Clean Utilization, Kunming 650093, Yunnan, China.
[2]School of Minerals Processing and Bioengineering, Central South University, Changsha 410083, Hunan, China.
[3]College of Chemistry and Chemical Engineering, Southwest Petroleum University, Chengdu 610500, Sichuan, China.

Correspondence to: Prof. Lei Xie, School of Minerals Processing and Bioengineering, Central South University, No.932 South Lushan Road, Changsha 410083, Hunan, China. E-mail: lei.xie@csu.edu.cn

Abstract

Understanding the interfacial interaction mechanisms of bubble-mineral systems is of paramount importance in the fields of fundamental science and engineering. Over the past few decades, researchers have employed the techniques such as atomic force microscope colloidal or bubble probe to quantitatively measure the bubble-mineral and bubble-bubble interactions at the nanoscale. However, accurately quantifying the interactions involving deformable bubbles has proven challenging due to the complexity of both theoretical analysis and experimental verification. To improve the understanding of interfacial mechanisms involved in the bubble and mineral systems, an overview of recent nanomechanical advancements in bubble-mineral interaction is required. In this review, we provide a comprehensive review of recent advancements in the nanomechanical understanding of interactions of bubble-mineral particles or surfaces and the interactions of bubble-bubble in mineral systems during various interfacial processes. Furthermore, we highlight the potential challenges for future research in this area. By shedding light on the underlying mechanisms governing interfacial interactions in bubble-mineral systems, this review offers valuable insights and paves the way for the development of effective strategies to manipulate and control these interactions in both environmental and engineering applications.

Keywords: Bubble-mineral systems, hydrophobic interaction, atomic force microscope, bubble probe

INTRODUCTION

Minerals play a crucial role in providing essential inorganic materials and are integral components in numerous engineering and technological applications. The interfacial interaction of bubble-mineral systems holds immense importance in engineering contexts, such as carbon dioxide sequestration[1], flotation separation[2], environmental protection, and drug delivery[3]. In the environmental domain, for instance, many clay minerals have the ability to capture and store CO_2, thereby influencing the mineralization process and exerting a significant impact on global warming and the carbon cycle[4]. In the realm of minerals processing, froth flotation entails the generation of bubbles that capture hydrophobic mineral particles within a slurry.

Subsequently, the resulting bubble-particle aggregates rise to the surface of the slurry under the influence of buoyancy, thereby enabling the targeted separation of mineral particles exhibiting diverse wettabilities[5]. However, the majority of natural minerals possess hydrophilic crystal planes that generally exhibit limited interactions with bubbles[6]. Only a handful of minerals, including graphite, molybdenite, talc, and chalcopyrite, demonstrate the inherent hydrophobic properties[7,8]. Additionally, hydrophilic minerals adsorbed with surfactants (e.g., collectors) can expose nonpolar chains, effectively rendering them hydrophobic[8,9]. In these cases, the attractive interaction between bubbles and minerals is significantly enhanced, leading to an increased tendency of attachment[10,11]. Such attraction is commonly attributed to the hydrophobic interaction[12]. From both fundamental and practical standpoints, unraveling the physics underlying interfacial interaction mechanisms of bubble-mineral systems, particularly for hydrophobic interaction, is of vital significance. This knowledge holds tremendous promise for effectively modulating the interfacial interactions of bubble-mineral systems in engineering applications, thereby paving the way for innovative solutions in these domains.

Hydrophobic interactions play a crucial role in aqueous systems, as they represent a strong attraction between nonpolar substances. Research in this area has garnered significant attention. Although the observation of hydrophobic interaction dates back to 1937[13], its first quantification was not conducted until 1982 by Israelachvili and Pashley[14]. In their seminal work, the hydrophobic interaction between two hydrophobic surfaces in aqueous solution at short-range distances (0.1-10 nm) was accurately determined. They found that this force followed a single exponential decay model: $\frac{F_{HB}}{R} = -C_0 \exp(-D/D_0)$, where R (m) is the radius of interacting surfaces, C_0 (J·m^{-2}) is a parameter related to interfacial energy, and D (m) and D_0 (m) are the separation distance and decay length, respectively[14]. Several studies have demonstrated that the decay length of hydrophobic interaction could be affected by surface characteristics and solution conditions, with a larger D_0 value indicating a stronger hydrophobic interaction[15-17]. Donaldson *et al.* later reported another expression for the surface interactions of the same materials: $\frac{F_{HB}}{R} = -2\gamma_i H_y \exp(-D/D_0)$, where $H_y = 1 - \frac{a_0}{a}$ is a nondimensional hydra parameter with a_0 and a indicating the hydrophilic and hydrophobic areas, respectively, and γ_i is the interfacial tension[18]. Remarkably, this equation can explain both the hydrophobic interaction ($0 < H_y \leq 1$) and hydration force ($H_y < 0$) between two heterogeneous surfaces.

The recognition that hydrophobic interaction is a short-range attractive force closely linked to the structuring of water is widely accepted[19]. However, the hydrophobic interactions reported have exhibited attraction with different ranges, which may indicate the complex origins of hydrophobic interaction. Faghihnejad and Zeng's model has successfully explained the hydrophobic interactions of different ranges[20]: (I) a long-range attraction (~20 to hundreds of nm): the electrostatic effect of local charge fluctuations or the bridging of micro- and submicroscopic bubbles; (II) an intermediate-range attraction (several to ~20 nm): the bridging of nanobubbles or the Grotthuss effect; and (III) a short-range attraction

(< 1 to several nm): the rearrangement of water molecules near hydrophobic surfaces. Therefore, the attraction for the first two cases is not attributed to the hydrophobic interaction, while the attraction for the last case is considered to be governed by the intrinsic hydrophobic interaction.

The atomic force microscope (AFM), a prominent nanomechanical tool, has been extensively utilized to quantify the intermolecular and surface forces, resulting in the significant advancements in understanding the interaction mechanism of solid surfaces in aqueous media[17,21,22]. However, when it comes to the measurements of deformable bubbles, the complexity is amplified due to the practical challenges associated with manipulating deformable objects and accurately interpreting force results[23,24]. To address these challenges, researchers have developed the AFM colloidal probe and bubble probe techniques to explore the interactions between bubbles and mineral systems[25-27]. These investigations have revealed the intriguing findings: the van der Waals (VDW) or electrostatic double layer (EDL) forces sustain the stable water film confined between bubbles and hydrophilic surfaces, while the hydrophobic interaction triggers the water film rupture and promotes the bubble attaches to hydrophobic substrates[21,22,25,28]. Additionally, it has been found that the factors such as the density and speciation of surface functional groups, presence of surfactants, solution salinity, and surface roughness could significantly influence the dewatering process of water films during the approach between bubbles and surfaces[5,23,29,30].

Although there has been a large number of great literature surveys on hydrophobic interactions involving mineral systems[5,7,24], there is a notable absence of literature review efforts specifically targeting the mechanisms of interfacial interactions of bubbles and mineral systems. This knowledge gap has significantly hindered our comprehension of these interactions within relevant environmental processes and engineering domains. The accurate quantification of interactions involving deformable bubbles in mineral systems is crucial for enhancing our comprehension of related interaction processes, uncovering the underlying mechanisms, and refining existing models while developing more efficient colloidal and interfacial technologies. In this review, we delve into the interfacial interaction mechanisms of bubble-mineral systems at the nanoscale, especially during mineral flotation. These interfacial interactions and phenomena are of paramount importance and have direct implications for water treatment, flotation separation, and many other engineering processes. Consequently, we present an exploration of cutting-edge nanomechanical techniques employed for quantifying the hydrophobic interaction and other surface forces. Furthermore, we delve into the recent progress in understanding the interplay of bubble and mineral systems, with a particular emphasis on their relevance to mineral processing. Additionally, we present the persisting challenges and provide a forward-looking for future research directions. Overall, this comprehensive review contributes to enhancing our understanding of the intricate interfacial interaction mechanisms within bubble-mineral systems at the nanoscale, thereby illuminating potential avenues for developing effective strategies that can manipulate the interaction behaviors of bubble-mineral systems.

COLLOIDAL FORCE MEASUREMENT TECHNIQUES
AFM colloidal probe and bubble probe techniques
Significant advances have been made with the successful implementation of AFM colloidal probe and bubble probe techniques to investigate the interactions within various surface systems involving bubbles under different conditions[25,31]. The AFM colloidal probe technique entails gluing a colloidal particle onto an AFM tipless cantilever, allowing the direct quantification of forces between colloidal particles and surface-attached bubbles [Figure 1A]. This technique has been widely employed in studying diverse colloidal systems in liquid media. Figure 1B illustrates a schematic of AFM bubble probes for direct force measurements with solid surfaces. To prepare the AFM bubble probe, the hydrophobized cantilever is gradually lowered towards a bubble until the bubble attaches to the cantilever. Subsequently, the cantilever
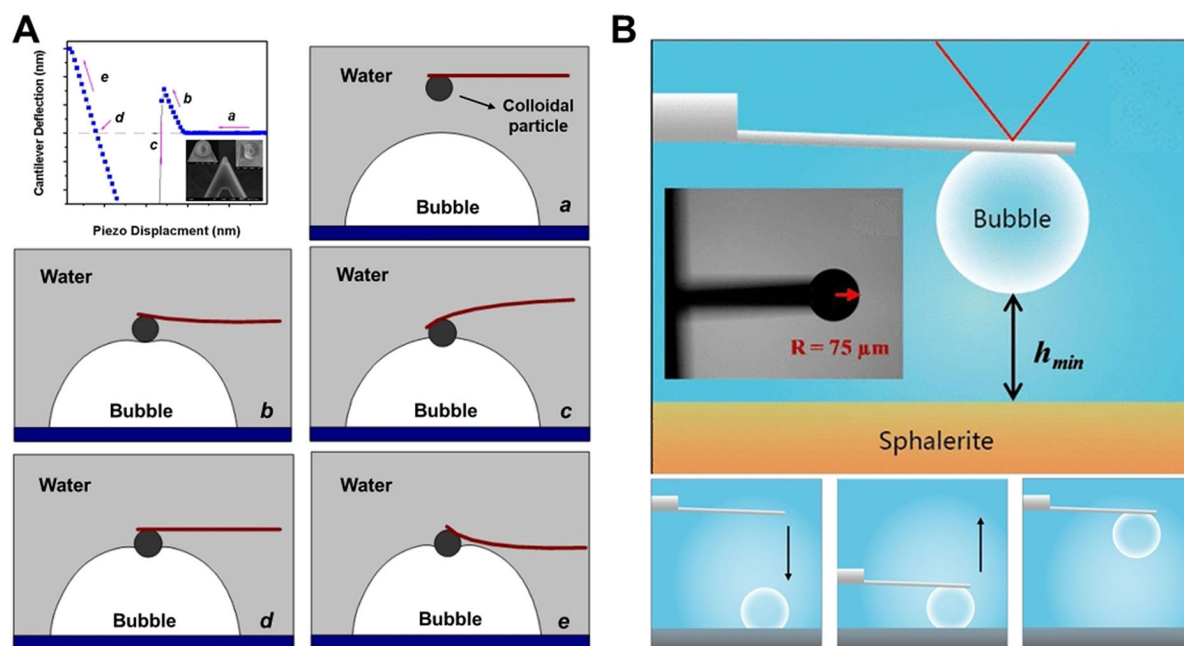
Figure 1. Schematic of AFM (A) colloidal probe and (B) bubble probe techniques. Reproduced from ref.[32] for (A), Copyright 2014, Elsevier; and from ref.[21] for (B), Copyright 2015, the American Chemical Society. AFM: Atomic force microscope.

is lifted to detach the bubble from the surface. The resulting AFM bubble probe is laterally maneuvered and precisely positioned above the substrate to facilitate the force measurements at a desired approach velocity.

Other force measurement techniques for bubble-involving systems

Surface forces apparatus (SFA) is another nanomechanical technique that could be used for measuring the interaction forces of bubbles. Originally designed for force measurements in vacuum or gas environments[33], SFA has undergone the subsequent redesign and improvements to enable the force quantification in complex aqueous media, facilitating the experimental demonstration of various surface forces, e.g., hydrophobic interactions[34]. In typical SFA measurements [Figure 2A], the absolute separation distance and surface deformation can be measured by a sophisticated optical method known as multiple-beam interferometry. This technique monitors the wavelength changes of the fringes of equal chromatic order (FECO)[35]. By analyzing the disparity between the driven distance and the observed change in surface separation through FECO patterns, the interaction forces can be quantified using Hooke's law. To investigate the bubble-surface interaction using SFA, Pushkarova *et al.* replaced a mica-coated cylinder with a bubble formed within a closed capillary tube[36,37]. To monitor the deformation of the bubble and the thickness of the film confined between the bubble and the mica surface, white light interferometry was employed[36]. The use of white light interferometry offers an advantage where it allows for the measurement of absolute separation distance without relying on light intensity at zero distance. It is important to note that no spring is utilized in the modified SFA configuration, and thus, the direct force measurement is impossible. During the force interpretation, Pushkarova *et al.*[36,38] simplified the analysis by treating the bubble as a Hookean linear spring with a spring constant approximately equal to the surface tension[39,40]. Later, Chan *et al.* established a more accurate relationship between the force used on the bubble and the degree of surface compression, illustrating that the "spring" is, in fact, nonlinear[41].
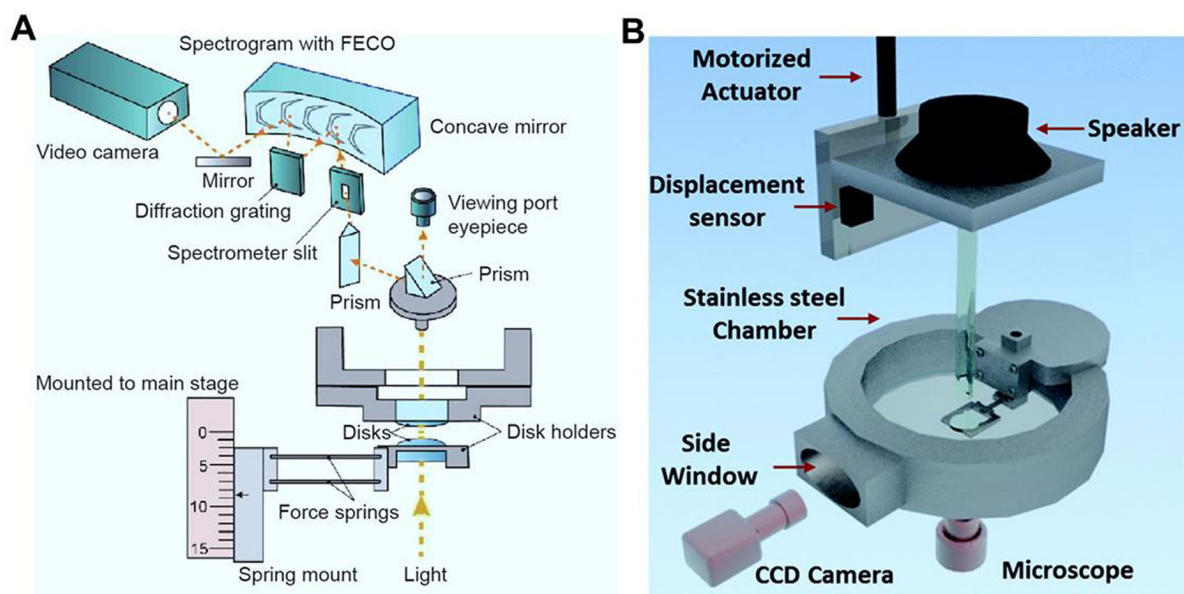
Figure 2. Schematic of (A) SFA and (B) ITLFFA techniques. Adapted from ref.[35] for (A), Copyright, 2021 Elsevier; and ref.[45] for (B), Copyright 2016, The Royal Society of Chemistry. CCD: Charge-coupled device; FECO: fringes of equal chromatic order; SFA: surface forces apparatus.

Both the nanomechanical AFM and SFA have traditionally been limited to experiments conducted at low Reynolds numbers ($R_e < 10^{-2}$). To investigate the interaction at intermediate Reynolds numbers ($10^{-2} < R_e < 10^2$), Pan *et al.*[42,43] developed the integrated thin film drainage apparatus (ITFDA) equipped with two perpendicularly positioned high-speed cameras to capture the detailed images of bubble deformation[44]. Moreover, it allows for accurate calculation of capillary forces that arise after contact line formation. Recently, Zhang *et al.* have extended the capabilities of the original ITFDA by introducing the integrated thin liquid film force apparatus (ITLFFA) [Figure 2B], which enables simultaneous measurements of both the interaction and water film profiles over higher Reynolds numbers[45]. To achieve this, they replaced the glass sphere with a transparent glass plate and placed the measurement cell on an inverted microscope. By utilizing a dual-wavelength interference technique, the absolute separation distance was able to be precisely measured[46].

In 2016, the force measurement apparatus for deformable surfaces (FADS) was designed by Pan *et al.* to analyze the dynamic profile of thin water film and bubble-surface interactions[42]. To carry out the measurements, a liquid cell consisting of two closely spaced silica plates without direct mechanical connection was utilized. The lower plate was designed to be adjustable in position, allowing for moving up or down at a desired approach velocity through the piezoelectric actuators. Within the FADS system, the interaction can be directly measured while driving a bubble to approach the specially designed flat cantilever submerged in water[42]. Through the integration of monochromatic interferometry and a high-speed camera, a remarkable synchronization has been achieved between direct force measurement and spatiotemporal profile. Moreover, a side-view camera was incorporated into the setup to capture the variation in dynamic contact angle. Notably, FADS was capable of measuring the forces with non-transparent substrates by positioning a bubble beneath the substrate within an inverted microscope configuration.

Theoretical analysis

The complex interplay among surface forces, hydrodynamic forces, and bubble deformation can be accurately described by the Stokes-Reynolds-Young-Laplace (SRYL) model[24]. Of particular importance, the tangentially immobile boundary conditions at the interfaces between the bubble and substrate are assumed during the interactions. Consequently, the dewatering process of a confined water film between the bubble and substrate can be depicted employing Reynolds lubrication theory, as shown in Equation 1[25]:

$$\frac{\partial h(r, t)}{\partial t} = \frac{1}{12\mu r}\frac{\partial}{\partial r}\left(rh^3\frac{\partial p(r, t)}{\partial r}\right) \tag{1}$$

where $h(r, t)$, μ, r, and $p(r, t)$ are the water film thickness (m), water viscosity (Pa·s), radical coordinate (m), and the excessive hydrodynamic pressure in the water film relative to a bulk solution (Pa), respectively.

The bubble deformation in response to the Laplace pressure, hydrodynamic pressure, and disjoining pressure can be depicted by the Young-Laplace equation, as presented in Equations 2-5[47]:

$$\frac{\gamma}{2r}\frac{\partial}{\partial r}\left(r\frac{\partial h(r, t)}{\partial r}\right) = \frac{2\gamma}{R_b} - p(r, t) - \Pi[h(r, t)] \text{ (bubble-bubble)} \tag{2}$$

$$\frac{\gamma}{r}\frac{\partial}{\partial r}\left(r\frac{\partial h(r, t)}{\partial r}\right) = \frac{2\gamma}{R_b} - p(r, t) - \Pi[h(r, t)] \text{ (bubble-plane)} \tag{3}$$

$$\frac{\gamma}{r}\frac{\partial}{\partial r}\left(r\frac{\partial h(r, t)}{\partial r}\right) = \frac{2\gamma}{R_{pb}} - p(r, t) - \Pi[h(r, t)] \text{ (bubble-particle)} \tag{4}$$

$$\bar{R}_{bp} = (1/R_b + 1/R_p)^{-1} \tag{5}$$

where γ is the interfacial tension (N·m⁻¹), R_b and R_p are the radii of bubbles and particles (m), and $\Pi[h(r, t)]$ is the overall disjoining pressure in the confined thin water film (Pa). Disjoining pressure refers to the additional pressure within a confined space relative to a bulk phase, which arises from surface forces[21]. According to the classical Derjaguin-Landau-Verwey-Overbeek (DLVO) theory, the stability of a colloidal system is governed by VDW and EDL forces. If the DLVO interaction provides a repulsive energy barrier to prevent the approach of colloidal particles, the colloidal system will be stable.

The disjoining pressure of VDW interaction $\Pi_{VDW}[h(r, t)]$ (Pa) is related to the Hamaker constant (A_H, J), which could be calculated by Equation 6[48]:

$$\Pi_{VDW}[h(r, t)] = -\frac{A_H}{6\pi h^3} \tag{6}$$

It should be mentioned that Equation 6 is a coarse approximation for calculating the Hamaker constant. To obtain a more precise value of the Hamaker constant, full spectral information for the dielectric function and refractive index should be used[49].

The disjoining pressure of EDL interaction $\Pi_{EDL}[h(r, t)]$ (Pa) in bubble-bubble or plane interaction systems can be described by Equations 7 and 8[24], respectively.

$$\Pi_{EDL}[h(r, t)] = 64 k_B T \rho_0 \tanh^2 \left(\frac{e\varphi_b}{4 k_B T} \right) e^{[-\kappa h]} \tag{7}$$

$$\Pi_{EDL}[h(r, t)] = \frac{2\varepsilon_0 \varepsilon \kappa^2 \left[(e^{+\kappa h} + e^{-\kappa h}) \psi_b \psi_s - (\psi_b^2 + \psi_s^2) \right]}{(e^{+\kappa h} - e^{-\kappa h})^2} \tag{8}$$

where the Boltzmann constant (k_B, J·K^{-1}), representing the fundamental relationship between temperature and energy, is denoted. The surface potentials of the bubble (φ_b, V) and the plane (φ_s, V) are included as variables pertaining to their respective electrostatic properties. The parameter ρ_0 signifies the number density of ions in the surrounding aqueous solution, while e denotes the charge of an electron. The vacuum permittivity (ε_0, F·m^{-1}) and the dielectric constant (ε, F·m^{-1}) are taken into consideration, alongside the reciprocal value of the Debye length (κ, m^{-1}). It is noted that both the constant charge and constant potential boundary conditions are limiting cases. In reality, one of the two interacting surfaces could have the charge regulation, thereby resulting in the forces to lie between these two boundary conditions[50].

The presence of hydrophobic and other possible attractive interactions (e.g., bridging interactions due to polymers) can possibly overcome the energy barrier, ultimately resulting in the aggregation of colloidal particles, which is generally referred to as the so-called extended DLVO (EDLVO) model[49]. Due to the scope of this review, only the hydrophobic role is discussed in this work.

The disjoining pressure of hydrophobic interaction $\Pi_{HB}[h(r, t)]$ (Pa) is always attractive and related to the decay length D_0 (m) and water contact angle θ_c (°), as described by Equation 9[28,51]:

$$\Pi_{HB}[h(r, t)] = -\frac{\gamma(1 - \cos\theta_c)}{D_0} \exp\left(-\frac{h}{D_0} \right) \tag{9}$$

Force measurements are normally carried out on curved surfaces in configurations such as a sphere *vs.* a plane and two spheres. Hence, for the large particles in which curvature does not substantially affect the integration, the overall interactions can be theoretically calculated by Equation 10 based on the Derjaguin approximation[52,53]:

$$F(t) = 2\pi \int_0^\infty [p(r, t) + \Pi(h(r, t))] r \, dr \tag{10}$$

BUBBLE-MINERAL PARTICLE INTERACTION

AFM colloidal probes have been widely used in nanomechanical quantification of interactions between particles and bubbles in liquid media. The pioneering quantifications of particle-bubble interactions were independently carried out by Butt[54] and Ducker *et al.*[55]. By driving the cantilever-attached glass sphere to approach a bubble immobilized on the substrate in an electrolyte solution, it was observed that bare glass spheres exhibited the pure repulsion due to DLVO forces, while the silane hydrophobized glass sphere displayed the snap-in behavior resulting from the hydrophobic interaction[54]. Besides, the interactions between bubbles and particles were also investigated using the cantilever attached to hydrophilic and hydrophobic silica particles[55]. Interestingly, both types of silica particles exhibited additional hydrophobic interactions; however, the introduction of sodium dodecyl sulfate (SDS) eliminated the long-range interaction[55]. Subsequently, Fielden *et al.* revisited the interaction between bubbles and silica particles[56], which revealed the rapid collapse of confined water films, particle attachment, and the formation of a three-

phase contact line for hydrophobic silica particles, consistent with the results obtained by the previous work[55]. On the other hand, the interaction between bubbles and hydrophilic silica particles was found to be monotonically repulsive, while the anomalous attraction reported in the previous work[55] most likely arose from the hydrophobic impurities[56].

Using the AFM colloidal probe technique, researchers have successfully quantified the interaction between a solid particle with varying chemistry and a bubble in complex aqueous solutions containing different reagents[23,29,57]. For example, a colloidal ZnS particle was fabricated to explore the interaction between ZnS and bubbles[58]. Through this examination, researchers observed a long-range repulsion between two entities, while the hydrophobic interaction at closer distances led to the particle-bubble attachment. The introduction of copper ions and subsequent dithiocarbonate noticeably diminished the obtained repulsion[58]. These findings have provided valuable insights into the intricate dynamics of bubble-particle interactions within diverse liquid environments.

Nguyen *et al.* conducted a comprehensive investigation into the hydrodynamic influence on particle-bubble interactions, employing AFM with varying approach velocities[59,60]. The interaction between glass spheres and bubbles was found to exhibit a monotonically repulsive behavior that could be intensified with increasing approach velocity. When the approach velocities remained below 0.6 μm$\cdot$s^{-1}, hydrodynamic forces can be deemed negligible, and surface forces played an important role. In contrast, when higher approach velocities were considered, the force measurements could be effectively explained by the modified Stokes law, which accurately accounted for the behavior at larger separation distances. In this regime, the influence of surface forces could be neglected. However, the detailed information on the film drainage and overall interfacial deformation cannot be acquired due to the difficulty of measuring the absolute separation distance by AFM.

Gillies *et al.* proposed an alternative approach to determine the absolute separation distance between a bubble and a particle during their interaction[61,62]. In their approach, the bubble was assumed to remain undeformed at larger distances under the combined effect of hydrodynamic and interaction forces. This approach relied on the notion that even soft bodies exhibited the behavior akin to rigid bodies when subjected to sufficiently weak interactions. Taran *et al.* subsequently utilized this approach to explore the time-dependent aspects of the interaction between silica particles and bubbles[63]. It is noteworthy that the limitation of this methodology is the requirement for independent measurement of surface potential while accurately determining the surface potential of bubbles remains challenging. Thus, the ongoing research aims to overcome this limitation and enable the more precise characterization of bubble-particle interactions.

Recently, the role of collectors in the interaction between bubbles and particles has been investigated using AFM colloidal probes [Figure 3][64]. As illustrated in Figure 3A and B, when a cantilever-attached glass particle approached a surface-immobilized bubble, the cationic dodecyltrimethylammonium bromide (DTAB) adsorbed on glass particles induced the hydrophobic interaction with the bubble. However, an increase in DTAB concentration led to the adsorption of DTAB molecules as a bilayer, causing the surface to revert back to a hydrophilic state [Figure 3C]. On the other hand, the anionic SDS was unable to adsorb onto the glass surface, and thus, the repulsive force always dominated the interactions between the bubble and particle [Figure 3D]. In instances involving hydrophobized glass substrates, the potency of hydrophobic interactions was observed to diminish or even vanish altogether upon the inclusion of DTAB and SDS. Subsequently, similar methods were employed to investigate the interaction between coal particles and bubbles in a dodecane and oleic acid solution[65].
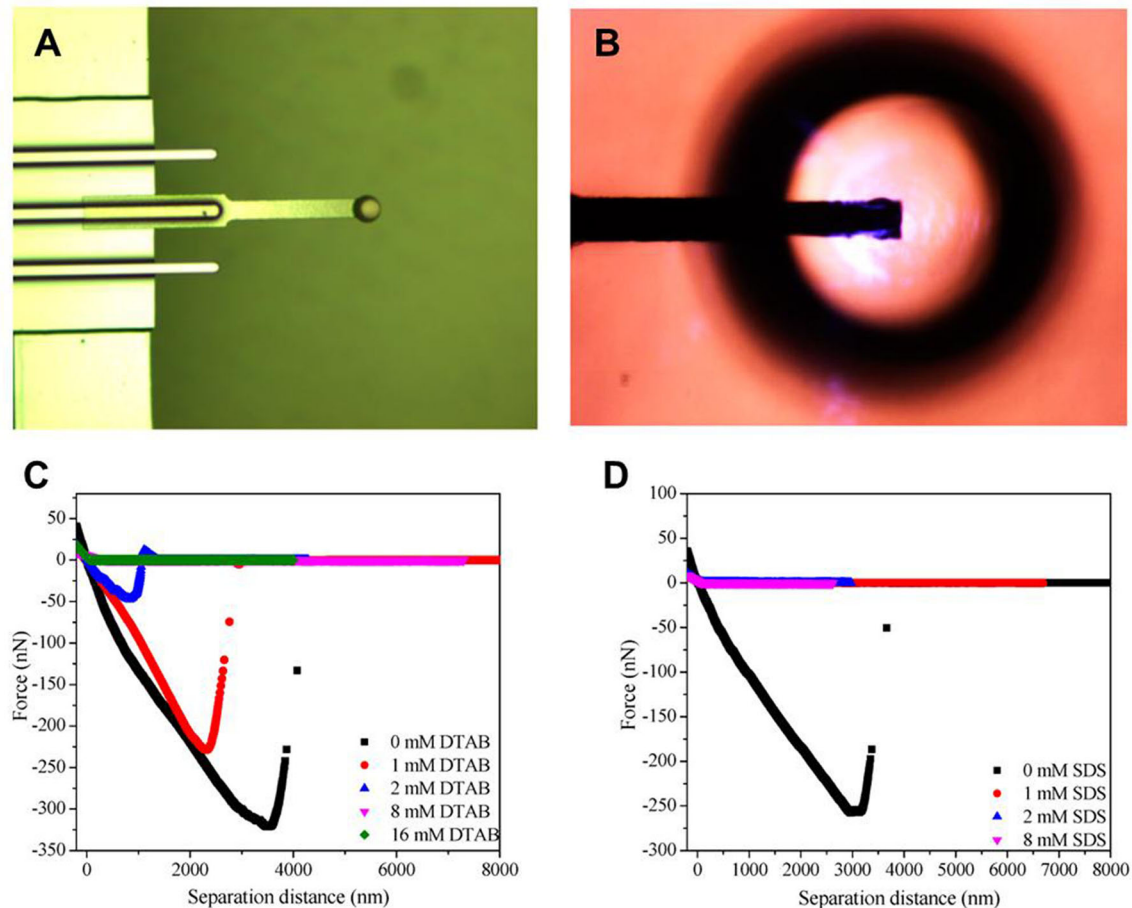
Figure 3. (A) AFM colloidal probe of glass microspheres; (B) Snapshot of bubble-particle interactions; Force-separation curves of interactions between hydrophobic glass microspheres and bubbles in (C) DTAB and (D) SDS solutions. Reproduced from ref.[64], Copyright 2018, MDPI. DTAB: Dodecyltrimethylammonium bromide; SDS: sodium dodecyl sulfate.

Despite the significant progress, performing the precise quantification of forces and the subsequent interpretation of force results pertaining to the bubble-natural mineral particle interactions continue to pose formidable challenges, primarily stemming from their inherent physical and chemical heterogeneities, including surface roughness, charge, and wettability. Surface roughness generally decreases the energy barrier from DLVO and EDLVO calculations, thereby enhancing the attachment efficiency of mineral particles to bubbles. However, surface roughness affects the wettability differently for hydrophilic and hydrophobic surfaces, i.e., the increase of surface roughness enhances the wettability of hydrophilic mineral surfaces but weakens the hydrophobic mineral surfaces. The presence of impurities in natural minerals introduces the heterogeneity in surface charge and wettability, which further affects the bubble-mineral particle interactions. To clarify the impact of surface nano-heterogeneities of minerals or bubbles on hydrophobic interactions in complex mineral systems, researchers have employed the theoretical calculation approaches[66-70]. These studies are valuable for predicting the particle adhesion behavior on bubble surfaces and assessing the effects of surface heterogeneities on hydrophobic interactions. It is worth noting that hydrophobic interactions play a crucial role in stabilizing the bubble-particle interaction systems[71]. The attachment process between bubbles and particles is dynamic, involving the deformation of bubbles and the dewatering of water film. The EDL and VDW interactions are typically not the dominant factor leading to the rupture of water film in bubble-particle systems, where these interactions are repulsive in such systems. Hence, the hydrophobic interaction has gained widespread recognition as the primary driving force behind

the rupture of confined thin water films. Notably, in the context of three-phase contact, the presence of surface nanobubbles induces a long-range attraction, which greatly enhances the bubble-particle interaction. As a result, this enhanced attachment stability considerably improves the overall stability of bubble-particle systems[72]. To quantify the stabilization of bubble-particle aggregation, researchers have turned to the utilization of the Bond number, which takes into account the contact angle[73].

BUBBLE-MINERAL SURFACE INTERACTION

Compared to bubble-mineral particle interactions, the force measurements on bubble-mineral surface interactions could directly employ the cleavage plane or polished surface of mineral particles, thereby successfully overcoming the operational challenges of mineral particles. Dynamic force apparatus (DFA) has been developed for investigating the fluid dynamic boundary conditions at mineral surfaces. Zhang *et al.* measured the spatial and temporal profiles of wetting film and the dynamic interactions between bubbles and functionalized silica/mica with various wettabilities in KCl solutions of different concentrations [Figure 4A][74]. Their findings demonstrated that the dimple of the bubble while approaching the hydrophobic surface was formed at a thinner water film thickness than that for the hydrophilic surface, and then, the water film drained more rapidly on hydrophobic surfaces compared to hydrophilic ones [Figure 4B-D]. For instance, on a silica surface with a contact angle of 36° [Figure 4C], it took approximately 8 s for the water film to be drained, while this process became even shorter (less than 1 s) for a silica surface with a contact angle of 90° [Figure 4D]. On both surfaces, the water films were unstable and ruptured at the edges of obstacles. In contrast, the hydrophilic silica required ~2 min to establish a flat and stable thin water film. The findings unequivocally highlighted the positive correlation between the hydrophobicity of silica surface and the magnitude of boundary slip, accentuated by higher approach velocities. Evidently, such fluctuations in slip length can be ascribed to the omnipresence of nanopores and nanobubbles embellishing solid surfaces, acting as pivotal agents in dictating the interfacial dynamics.

The AFM bubble probe technique offers a direct means of measuring the forces between a cantilever-attached bubble and a mineral surface in an aqueous environment. This technique provides certain advantages over the AFM colloidal probe technique, as smooth and flat mineral surfaces can be easily prepared through cleavage or polishing methods[26,27,75]. Utilizing the AFM bubble probe technique, the interactions between bubbles and mineral surfaces were quantitatively analyzed, and the SRYL theoretical model was used to calculate the separation distance (i.e., confined thin water film thickness) between the bubble and substrate[27]. However, due to the deformation exhibited by the bubbles during these experiments, conducting the simultaneous measurements of interaction and separation distance between bubbles and substrate surfaces remained challenging.

Recently, Shi *et al.* introduced a groundbreaking approach by combining reflection interference contrast microscopy (RICM) with the AFM bubble probe, enabling the simultaneous measurements of interactions and confined thin water film profiles between bubbles and mica surfaces[21]. The experimental setup, as depicted in Figure 5A, allowed for the visualization of fringe patterns resulting from the interference between monochromatic light reflections at the bubble/water and water/mica interfaces using RICM. Analysis of these fringe patterns provided insights into the spatiotemporal evolution of thin water film trapped between the bubble and the mica surface, allowing for the determination of its thickness, $h(r, t)$[76]. The AFM-RICM experimental results exhibited excellent agreement with theoretical calculations by the SRYL model, which considered the influence of disjoining pressure. Notably, the RICM interference fringe patterns revealed a central flattened region with a radial extent of 2 μm and a stable thin water film with a minimum thickness of ~7 nm during the approach of bubbles to bare mica surfaces [Figure 5B and C]. Furthermore, the jump-in behaviors of the bubble were observed for both mica surfaces with contact angles
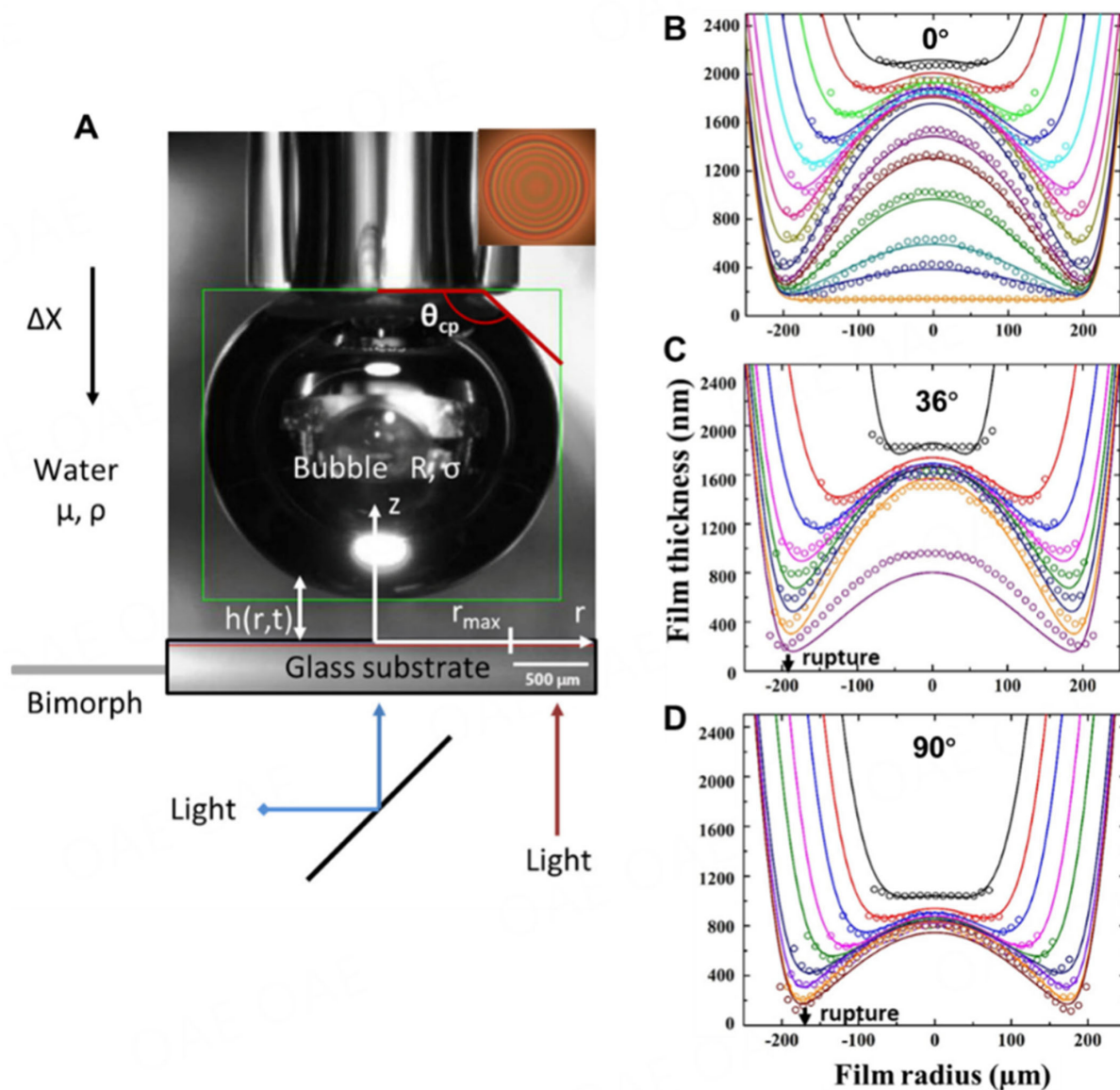
Figure 4. (A) schematic of an experimental setup for DFA; (B-D) Calculated water film thickness when an air bubble (R ~1.2 mm) approached (B) a hydrophilic silica surface with a contact angle of 0° and (C, D) a hydrophobic silica surface with contact angles of 36° and 90°, respectively. Reproduced from ref.[74], Copyright 2018, the American Chemical Society. DFA: Dynamic force apparatus.

of 45° and 90°, with the stronger bubble attachment observed on the substrate with higher hydrophobicity. These findings highlight the utility of AFM bubble probes combined with the RICM technique as a valuable tool for unraveling the complexities of bubble-surface interaction mechanisms.

The hydrophobicity of mineral surfaces plays a critical role in the bubble-mineral interactions[77], and the changes in the pulp environment, such as pH change or the addition of flotation reagents, have a significant effect on the hydrophobicity of mineral surfaces. Surface hydrophobicity adjustment is a commonly used strategy in flotation processes. In the selective flotation of molybdenum sulfide ores, molybdenite is naturally hydrophobic, and organic polymers are often utilized to depress the surface hydrophobicity[77]. In a recent investigation, the impact of polymer adsorption, specifically guar gum, on the bubble-molybdenite
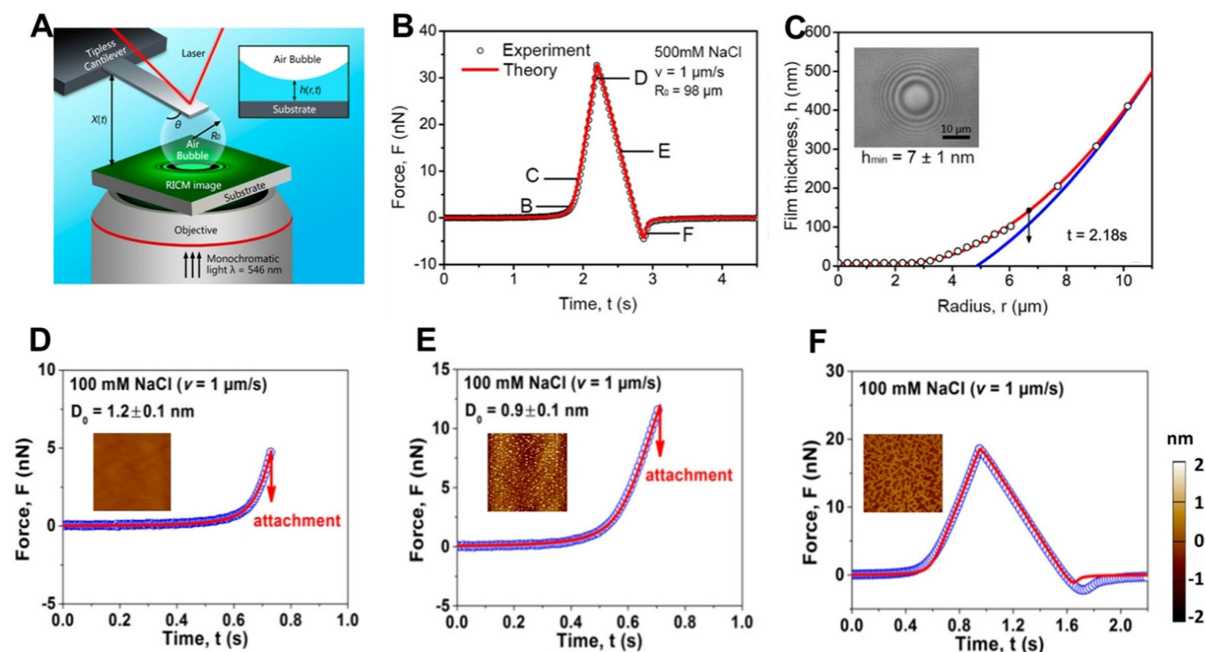
Figure 5. (A) schematic of experiment setup for AFM bubble probes coupled with RICM; (B) Time variation of the force between a bubble and a bare mica surface; (C) Water film profile at point D in panel B. Interaction force curves between a bubble and a molybdenite surface treated in (D) 0, (E) 1, and (F) 5 ppm guar gum. The open symbols are experimental results obtained from AFM measurements, and the solid curves are theoretical calculations. Inset: Corresponding AFM images (5 μm × 5 μm) of a molybdenite surface treated in 0, 1, and 5 ppm guar gum. Reproduced from ref.[21] for (A-C), Copyright 2015, the American Chemical Society; and ref.[27] for (D-F), Copyright 2017, the American Chemical Society. AFM: Atomic force microscope; RICM: reflection interference contrast microscopy.

surface interaction was explored[27]. In the absence of polymers [Figure 5D], the bubble exhibited a strong attachment to molybdenite surfaces, with a D_0 value of approximately 1.2 nm, characterizing the hydrophobic interaction. However, when molybdenite was conditioned with 1 ppm polymer, the surface displayed the randomly distributed aggregates with sparse polymer coverage of around 5.6% [Figure 5E]. Consequently, the weakened hydrophobic interaction led to the reduced bubble attachment to a mineral surface (D_0 = 0.9 nm). Notably, Figure 5F demonstrated the formation of an interconnected network structure among the adsorbed guar gum, resulting in approximately 44.5% polymer coverage after conditioning the mineral surface in 5 ppm guar gum. The additional repulsion, presumed to arise from the steric effect between the extended polymer chains and bubble surfaces, effectively inhibits the bubble attachment. These measured interaction results were found to be consistent with the observed flotation recovery of molybdenite. Furthermore, the interaction and attachment between bubbles and sphalerite surfaces were also investigated, and the bubble-sphalerite interaction was affected by hydrodynamic conditions, reagent addition, and ion concentration and types[26].

The AFM bubble probe offers a versatile approach to quantifying the interactions between bubbles and mineral surfaces in complex fluids, allowing for its widespread application across various mineral systems and related engineering applications. As a remarkable example of integrating fundamental research and practical implication, further exploration into characterizing the surface properties and interaction mechanisms of mineral surfaces can greatly contribute to establishing a comprehensive understanding of the correlation between basic intermolecular and surface interactions at the interfaces of bubbles, water, and minerals, with the overall separation performances on a macroscopic scale within the mineral processing industry, including the critical factors such as bubble-mineral attachment, flotation recovery, and selectivity.

BUBBLE-BUBBLE INTERACTION IN MINERAL SUSPENSION

Bubble coalescence and the associated interactions in mineral suspensions are of utmost importance in various engineering processes, such as mineral recovery and the oil industry. Understanding the hydrodynamic factors affecting the bubble coalescence and differential inhibition behaviors of monovalent (e.g., Na^+) and divalent cations (e.g., Ca^{2+} and Mg^{2+}) based on the partitioning of hydrated ions at the gas/liquid interface is crucial for realizing the efficient separation of mineral particles[78]. The highly hydrated divalent Mg^{2+} ions strongly influence the hydrogen bond network in water, leading to a locked configuration between cations and anions. This robust hydrogen bond network exhibits the remarkable stability against increasing the hydrodynamic stresses. Conversely, the less hydrated monovalent Na^+ ions have a relatively weak impact on the hydrogen bond network, and the air/liquid interface may become destabilized under the escalating hydrodynamic stresses, resulting in the bubble coalescence even at high electrolyte concentrations. The force measurements between two bubbles offer valuable insights into the bubble-bubble interaction and stability within colloidal systems. Moreover, the pH of a solution and the type of gas employed have been found to play a key role in determining the coalescence behavior of bubbles during the bubble-bubble interactions [Figure 6A][79]. The findings indicated that the air bubbles tended to coalesce at pH 4.0 and 5.5, whereas stable thin water films were formed at pH 7.0 and 10.3 [Figure 6B]. Across all inert gases studied (i.e., Ar and N_2), there existed a comparable pH range (pH 3-7) within which the bubble coalescence occurred, while the coalescence region for air appeared to be narrower compared to that of inert gases. Interestingly, CO_2 bubbles exhibited an anomalous stability, as they did not undergo the coalescence below pH 6 [Figure 6C].

In a previous study, Cui *et al.*[80] utilized the AFM bubble probe technique to measure the bubble-bubble interaction[72]. Figure 6D illustrates the interaction profile measured between two bubbles with a radius of 65 μm at a driving velocity of 1 μm·s^{-1} in 1 mM NaCl solution at pH ~5.6. A strong repulsion was observed as the bubbles approached each other, preventing the coalescence even at a maximum load of 15 nN. In aqueous solutions, VDW interactions are typically attractive with the Hamaker constant A_H ~3.73 × 10^{-20} J, contributing positively to the bubble coalescence. However, the calculated Debye length κ^{-1} was found to be 9.6 nm in 1 mM NaCl, indicating the presence of EDL repulsion between the bubbles. The SRYL model was employed for theoretical fitting, revealing that the surface potential of the bubbles was measured at -33 ± 4 mV. As illustrated in Figure 6E, the disjoining pressure originating from EDL repulsion outweighed that arising from VDW and hydrophobic interactions, thereby governing the bubble-bubble interaction and sustaining the confined thin water film. Figure 6F depicts the deformation of bubbles during the interaction. The bubbles are locally flattened on the maximum repulsion (external load), with a stable water film of approximately 17.8 nm confined in between, where the overall disjoining pressure is balanced by Laplace pressure.

Studies in the past have explored the impact of various hydrodynamic factors, such as the velocity at which bubbles approach each other, the angle of collision, and the hydrodynamic interfacial mobility, on their coalescence behaviors[81]. A pioneering study conducted by Kirkpatrick and Lockett[82] back in 1974 demonstrated the effect of approaching velocities on the collision dynamics between a rising bubble and a water/air interface. At high approaching velocities, bouncing behaviors were observed, while coalescence took place under low approaching velocities. In a more recent investigation, the collision between a rising bubble and a stationary bubble was meticulously examined through the utilization of a copper cap. The findings elucidated that off-center collisions exhibited a markedly higher probability of coalescence in comparison to head-on collisions[83]. This finding aligns with a previous report on the enhanced coalescence (demulsification) of emulsion drops, wherein off-center collisions were found to facilitate the interfacial shearing upon contact[84]. Thus, the observations regarding the bubble-bubble coalescence are consistent with the enhanced demulsifying effects observed through off-center collisions.
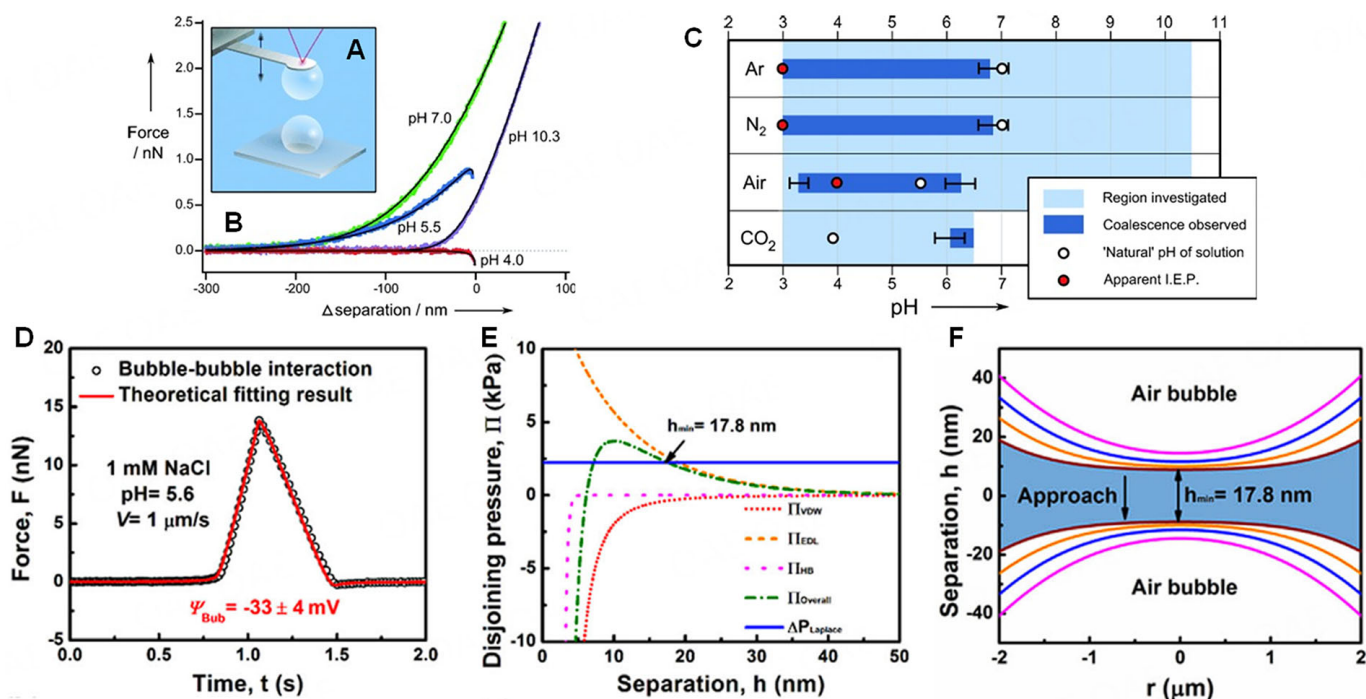
Figure 6. (A) Schematic of the force measurements between two bubbles using AFM bubble probes; (B) Force-separation curves between two air bubbles in different pH conditions; (C) The measured pH range of bubble coalescence for different types of gases; (D) Time variation of the force between two bubbles (radius ~65 μm) at an approach velocity of 1 μm·s^{-1} and the theoretical fitting results; (E) The disjoining pressure in a thin liquid film between two approaching bubbles caused by surface interactions; (F) The profiles of two approaching bubbles as the function of separation distance. The open symbols are the experimental data, and the solid curves are the theoretical data. Reproduced from ref.[79] for (A-C), Copyright 2011, John Wiley & Sons, Inc.; and from ref.[80] for (D-F), Copyright 2017, John Wiley & Sons, Inc. AFM: Atomic force microscope.

Very recent investigations have delved into the interactions between free-rising bubbles and both clean (mobile) and immobile liquid-air interfaces, with the latter being covered by a monolayer of surfactant[85,86]. The findings highlight the significant influence of liquid/gas interface mobility on the collision and coalescence behaviors of bubbles. Specifically, when the bubbles collided with mobile interfaces, a robust series of bouncing behaviors were observed prior to rapid coalescence, in stark contrast to the cases involving immobile interfaces. Experimental results revealed that the bubbles exhibited much stronger rebounding (up to 1.8 times the initial distance) when interacting with a clean mobile interface compared to an immobile interface. This enhanced rebounding behavior in the mobile interface scenario can be attributed to the lower levels of viscous dissipation during collisions, a conclusion further supported by numerical simulations. Previous investigations utilizing surface force measurements and rising bubble collision tests have provided quantitative and valuable insights into the roles played by surface forces (or disjoining pressure), hydrodynamic conditions, and interfacial properties in the bubble interactions. These findings hold significant implications for the stability and coalescence behaviors of bubbles across a wide range of industrial processes, including but not limited to pharmaceutics, food production, environmental applications, and mineral processing.

CONCLUSION

In this study, we have conducted a systematic review to highlight recent advancements in the nanomechanical understanding of interactions between bubble-mineral particles or surfaces and interactions between bubbles in mineral systems during various interfacial processes. Over the past few decades, significant efforts have been dedicated to investigating the interactions within bubble-mineral

systems, underscoring the crucial role of hydrophobic interactions. These interactions have gained widespread recognition as the primary driving force behind the rupture of confined thin water films. It is important to note that surface heterogeneity plays a substantial role in modulating the interaction between bubbles and mineral systems. However, accurately quantifying interactions involving deformable bubbles has proven to be challenging due to the inherent complexity of both theoretical analysis and experimental verification. Nonetheless, the field of colloidal force measurement techniques has flourished, employing a range of tools such as Atomic Force Microscopy, SFA, and interfacial tensiometer for liquid-liquid force measurements (ITLFFA) to characterize bubble and mineral system interactions at the nanoscale. Despite significant progress made in recent decades regarding our understanding of bubble-mineral and bubble-bubble interactions, there is still much work to be done in order to comprehensively unravel the quantitative mechanisms underlying these interactions at the nanoscale. Critical challenges persist, and further improvements are necessary for the novel nanomechanical tools alongside other methods such as high-resolution analytical techniques and theoretical simulations. These advancements will enable the development of effective strategies to modulate the interfacial processes on minerals and extend to other solid substances in fields such as chemical, environmental, and materials engineering.

Perspective

Based on the recent research breakthroughs, several key aspects remain to be fully elucidated:

(1) The precise physicochemical principles governing the hydrophobic interactions at different bubble-mineral and bubble-bubble interfaces have yet to be fully understood. Future studies should systematically investigate the formation and stability of interfacial bubbles and the interaction mechanisms under specific ion effects, particularly on mineral surfaces with varying hydrophobicity, chemistry, and structures.

(2) The correlation between interfacial properties (e.g., interfacial tension, interfacial rheology) and thin film dynamics during bubble-mineral and bubble-bubble interactions requires further exploration. The mobility of adsorbed components on bubbles and mineral surfaces can influence their properties and induce local variations in interfacial concentrations.

(3) The impact of hydrodynamic properties and flotation reagents on bubble-mineral and bubble-bubble interactions within complex mineral suspension systems remains an important area of research. Studies on bubble-bubble interactions and coalescence in the presence of fine mineral particles are still lacking. The extension of quantitative measurements of hydrophobic interactions from relatively simple systems to more complex ones represents an intriguing topic for investigation.

In conclusion, while challenges persist in understanding bubble-mineral and bubble-bubble interactions, it is encouraging to note that current research provides hope for a deeper understanding of practical systems in the near future. It is anticipated that with the ongoing development of measuring techniques, advanced functional methods will be devised to accurately quantify bubble-mineral and bubble-bubble interactions across a range of complex systems and scales. Integrating these techniques into colloidal predicaments within practical complex systems, coupled with optimizing models through machine learning approaches, will undoubtedly yield advantageous insights for both natural and industrial systems entailing bubble interactions.

DECLARATIONS

Authors' contributions

Data curation, interpretation, writing - original draft preparation, writing - reviewing and editing: Wang Z

Writing - reviewing: Xiang Y, Wang J, Gao Z, Sun W
Conceptualization, methodology, supervision, funding acquisition, project administration, writing - reviewing and editing: Xie L

Availability of data and materials
Not applicable.

Conflicts of interest
All authors declared that there are no conflicts of interest.

Ethical approval and consent to participate
Not applicable.

Consent for publication
Not applicable.

REFERENCES

1. Wang S, Tao Z, Persily SM, Clarens AF. CO_2 adhesion on hydrated mineral surfaces. *Environ Sci Technol* 2013;47:11858-65. DOI PubMed
2. Demir-yilmaz I, Ftouhi MS, Balayssac S, Guiraud P, Coudret C, Formosa-dague C. Bubble functionalization in flotation process improve microalgae harvesting. *Chem Eng J* 2023;452:139349. DOI
3. Mura S, Nicolas J, Couvreur P. Stimuli-responsive nanocarriers for drug delivery. *Nat Mater* 2013;12:991-1003. DOI PubMed
4. Iglauer S, Pentland CH, Busch A. CO_2 wettability of seal and reservoir rocks and the implications for carbon geo-sequestration. *Water Resour Res* 2015;51:729-74. DOI
5. Xing Y, Gui X, Pan L, et al. Recent experimental advances for understanding bubble-particle attachment in flotation. *Adv Colloid Interface Sci* 2017;246:105-32. DOI
6. Drelich J, Chibowski E, Meng DD, Terpilowski K. Hydrophilic and superhydrophilic surfaces and materials. *Soft Matter* 2011;7:9804-28. DOI
7. Wang Z, Lu Q, Wang J, et al. Nanomechanical insights into hydrophobic interactions of mineral surfaces in interfacial adsorption, aggregation and flotation processes. *Chem Eng J* 2023;455:140642. DOI
8. Heyes G, Trahar W. The natural flotability of chalcopyrite. *Int J Miner Process* 1977;4:317-44. DOI
9. Wei Z, Sun W, Wang P, Han H, Liu D. The structure analysis of metal-organic complex collector: from single crystal, liquid phase, to solid/liquid interface. *J Mol Liq* 2023;382:122029. DOI
10. Bepete G, Anglaret E, Ortolani L, et al. Surfactant-free single-layer graphene in water. *Nat Chem* 2017;9:347-52. DOI
11. Lu Z, Zhu W, Yu X, et al. Ultrahigh hydrogen evolution performance of under-water "superaerophobic" MoS_2 nanostructured electrodes. *Adv Mater* 2014;26:2683-7. DOI PubMed
12. Xie L, Wang J, Lu Q, et al. Surface interaction mechanisms in mineral flotation: Fundamentals, measurements, and perspectives. *Adv Colloid Interface Sci* 2021;295:102491. DOI
13. Meyer EE, Rosenberg KJ, Israelachvili J. Recent progress in understanding hydrophobic interactions. *Proc Natl Acad Sci U S A* 2006;103:15739-46. DOI PubMed PMC

14.   Israelachvili J, Pashley R. The hydrophobic interaction is long range, decaying exponentially with distance. *Nature* 1982;300:341-2. DOI PubMed

15.   Cui X, Liu J, Xie L, et al. Modulation of hydrophobic interaction by mediating surface nanoscale structure and chemistry, not monotonically by hydrophobicity. *Angew Chem Int Ed Engl* 2018;57:11903-8. DOI PubMed

16.   Cui X, Liu J, Xie L, Huang J, Zeng H. Interfacial ion specificity modulates hydrophobic interaction. *J Colloid Interface Sci* 2020;578:135-45. DOI PubMed

17.   Ma CD, Wang C, Acevedo-Vélez C, Gellman SH, Abbott NL. Modulation of hydrophobic interactions by proximally immobilized ions. *Nature* 2015;517:347-50. DOI PubMed

18.   Donaldson SH Jr, Røyne A, Kristiansen K, et al. Developing a general interaction potential for hydrophobic and hydrophilic interactions. *Langmuir* 2015;31:2051-64. DOI

19.   Chandler D. Interfaces and the driving force of hydrophobic assembly. *Nature* 2005;437:640-7. DOI PubMed

20.   Faghihnejad A, Zeng H. Hydrophobic interactions between polymer surfaces: using polystyrene as a model system. *Soft Matter* 2012;8:2746-59. DOI

21.   Shi C, Cui X, Xie L, et al. Measuring forces and spatiotemporal evolution of thin water films between an air bubble and solid surfaces of different hydrophobicity. *ACS Nano* 2015;9:95-104. DOI

22.   Xie L, Wang J, Huang J, et al. Anisotropic polymer adsorption on molybdenite basal and edge surfaces and interaction mechanism with air bubbles. *Front Chem* 2018;6:361. DOI PubMed PMC

23.   Gillies G, Kappl M, Butt HJ. Direct measurements of particle-bubble interactions. *Adv Colloid Interface Sci* 2005;114-5:165-72. DOI PubMed

24.   Xie L, Shi C, Cui X, Zeng H. Surface forces and interaction mechanisms of emulsion drops and gas bubbles in complex fluids. *Langmuir* 2017;33:3911-25. DOI PubMed

25.   Cui X, Shi C, Xie L, Liu J, Zeng H. Probing interactions between air bubble and hydrophobic polymer surface: impact of solution salinity and interfacial nanobubbles. *Langmuir* 2016;32:11236-44. DOI PubMed

26.   Xie L, Shi C, Wang J, et al. Probing the interaction between air bubble and sphalerite mineral surface using atomic force microscope. *Langmuir* 2015;31:2438-46. DOI

27.   Xie L, Wang J, Yuan D, et al. Interaction mechanisms between air bubble and molybdenite surface: impact of solution salinity and polymer adsorption. *Langmuir* 2017;33:2353-61. DOI

28.   Shi C, Cui X, Zhang X, et al. Interaction between air bubbles and superhydrophobic surfaces in aqueous solutions. *Langmuir* 2015;31:7317-27. DOI

29.   Johnson DJ, Miles NJ, Hilal N. Quantification of particle-bubble interactions using atomic force microscopy: a review. *Adv Colloid Interface Sci* 2006;127:67-81. DOI PubMed

30.   Ralston J, Dukhin SS, Mishchuk NA. Wetting film stability and flotation kinetics. *Adv Colloid Interface Sci* 2002;95:145-236. DOI PubMed

31.   Shi C, Yan B, Xie L, et al. Long-range hydrophilic attraction between water and polyelectrolyte surfaces in oil. *Angew Chem Int Ed Engl* 2016;55:15017-21. DOI PubMed

32.   Ren S, Masliyah J, Xu Z. Studying bitumen-bubble interactions using atomic force microscopy. *Colloids Surf A Physicochem Eng Asp* 2014;444:165-72. DOI

33.   Tabor D, Winterton RHS. The direct measurement of normal and retarded van der Waals forces. *Proc R Soc Lond A* 1969;312:435-50. DOI

34.   Israelachvili JN, Pashley RM. Measurement of the hydrophobic interaction between two hydrophobic surfaces in aqueous electrolyte solutions. *J Colloid Interface Sci* 1984;98:500-14. DOI

35.   Zhang J, Zeng H. Intermolecular and surface interactions in engineering processes. *Engineering* 2021;7:63-83. DOI

36.   Pushkarova RA, Horn RG. Surface forces measured between an air bubble and a solid surface in water. *Colloids Surf A Physicochem Eng Asp* 2005;261:147-52. DOI

37.   Manica R, Connor JN, Clasohm LY, Carnie SL, Horn RG, Chan DY. Transient responses of a wetting film to mechanical and electrical perturbations. *Langmuir* 2008;24:1381-90. DOI PubMed

38.   Pushkarova RA, Horn RG. Bubble-solid interactions in water and electrolyte solutions. *Langmuir* 2008;24:8726-34. DOI PubMed

39.   Attard P, Miklavcic SJ. Effective spring constant of bubbles and droplets. *Langmuir* 2001;17:8217-23. DOI

40.   Attard P, Miklavcic SJ. Effective spring description of a bubble or a droplet interacting with a particle. *J Colloid Interface Sci* 2002;247:255-7. DOI PubMed

41.   Chan DYC, Manor O, Connor JN, Horn RG. Soft matter: from shapes to forces on the nanoscale. *Soft Matter* 2008;4:471-4. DOI PubMed

42.   Pan L, Yoon R. Measurement of hydrophobic forces in thin liquid films of water between bubbles and xanthate-treated gold surfaces. *Miner Eng* 2016;98:240-50. DOI

43.   Wang L, Sharp D, Masliyah J, Xu Z. Measurement of interactions between solid particles, liquid droplets, and/or gas bubbles in a liquid using an integrated thin film drainage apparatus. *Langmuir* 2013;29:3594-603. DOI PubMed

44.   Shahalami M, Wang L, Wu C, Masliyah JH, Xu Z, Chan DY. Measurement and modeling on hydrodynamic forces and deformation of an air bubble approaching a solid sphere in liquids. *Adv Colloid Interface Sci* 2015;217:31-42. DOI PubMed

45.   Zhang X, Tchoukov P, Manica R, Wang L, Liu Q, Xu Z. Simultaneous measurement of dynamic force and spatial thin film thickness

between deformable and solid surfaces by integrated thin liquid film force apparatus. *Soft Matter* 2016;12:9105-14. DOI

46.   Schilling J, Sengupta K, Goennenwein S, Bausch AR, Sackmann E. Absolute interfacial distance measurements by dual-wavelength reflection interference contrast microscopy. *Phys Rev E Stat Nonlin Soft Matter Phys* 2004;69:021901. DOI PubMed

47.   Chan DY, Klaseboer E, Manica R. Theory of non-equilibrium force measurements involving deformable drops and bubbles. *Adv Colloid Interface Sci* 2011;165:70-90. DOI PubMed

48.   Manica R, Chan DY. Drainage of the air-water-quartz film: experiments and theory. *Phys Chem Chem Phys* 2011;13:1434-9. DOI PubMed

49.   Israelachvili JN. Intermolecular and surface forces. 3rd ed. 2011. DOI

50.   Smith AM, Borkovec M, Trefalt G. Forces between solid surfaces in aqueous electrolyte solutions. *Adv Colloid Interface Sci* 2020;275:102078. DOI PubMed

51.   Tabor RF, Wu C, Grieser F, Dagastine RR, Chan DY. Measurement of the hydrophobic force in a soft matter system. *J Phys Chem Lett* 2013;4:3872-7. DOI

52.   Tabor RF, Grieser F, Dagastine RR, Chan DY. Measurement and analysis of forces in bubble and droplet systems using AFM. *J Colloid Interface Sci* 2012;371:1-14. DOI PubMed

53.   Bhattacharjee S, Elimelech M. Surface element integration: a novel technique for evaluation of DLVO interaction between a particle and a flat plate. *J Colloid Interface Sci* 1997;193:273-85. DOI PubMed

54.   Butt H. A Technique for measuring the force between a colloidal particle in water and a bubble. *J Colloid Interface Sci* 1994;166:109-17. DOI

55.   Ducker WA, Xu Z, Israelachvili JN. Measurements of hydrophobic and DLVO forces in bubble-surface interactions in aqueous solutions. *Langmuir* 1994;10:3279-89. DOI

56.   Fielden ML, Hayes RA, Ralston J. Surface and capillary forces affecting air bubble-particle interactions in aqueous electrolyte. *Langmuir* 1996;12:3721-7. DOI

57.   Preuss M, Butt H. Direct measurement of particle-bubble interactions in aqueous electrolyte: dependence on surfactant. *Langmuir* 1998;14:3164-74. DOI

58.   Gillies G, Kappl M, Butt HJ. Surface and capillary forces encountered by zinc sulfide microspheres in aqueous electrolyte. *Langmuir* 2005;21:5882-6. DOI PubMed

59.   Nguyen A, Nalaskowski J, Miller J. A study of bubble-particle interaction using atomic force microscopy. *Miner Eng* 2003;16:1173-81. DOI

60.   Nguyen A, Evans G, Nalaskowski J, Miller J. Hydrodynamic interaction between an air bubble and a particle: atomic force microscopy measurements. *Exp Therm Fluid Sci* 2004;28:387-94. DOI

61.   Gillies G, Prestidge CA, Attard P. Determination of the separation in colloid probe atomic force microscopy of deformable bodies. *Langmuir* 2001;17:7955-6. DOI

62.   Gillies G, Prestidge CA. Interaction forces, deformation and nano-rheology of emulsion droplets as determined by colloid probe AFM. *Adv Colloid Interface Sci* 2004;108-9:197-205. DOI PubMed

63.   Taran E, Hampton MA, Nguyen AV, Attard P. Anomalous time effect on particle-bubble interactions studied by atomic force microscopy. *Langmuir* 2009;25:2797-803. DOI PubMed

64.   Xing Y, Xu M, Li M, Jin W, Cao Y, Gui X. Role of DTAB and SDS in bubble-particle attachment: AFM force measurement, attachment behaviour visualization, and contact angle study. *Minerals* 2018;8:349. DOI

65.   Xu M, Xing Y, Cao Y, Gui X. Effect of dodecane and oleic acid on the attachment between oxidized coal and bubbles. *Minerals* 2018;8:29. DOI

66.   Gomez-flores A, Bradford SA, Hwang G, Heyes GW, Kim H. Particle-bubble interaction energies for particles with physical and chemical heterogeneities. *Minerals Engineering* 2020;155:106472. DOI

67.   Drelich JW, Bowen PK. Hydrophobic nano-asperities in control of energy barrier during particle-surface interactions. *Surf Innov* 2015;3:164-71. DOI

68.   Bargozin H, Hadadhania RA, Amiri TY. Influence of chemical heterogeneity and nanoscale roughness on the DLVO energy interaction by spherical coordinates. *J Dispers Sci Technol* 2016;37:806-15. DOI

69.   Bendersky M, Davis JM. DLVO interaction of colloidal particles with topographically and chemically heterogeneous surfaces. *J Colloid Interface Sci* 2011;353:87-97. DOI PubMed

70.   Shen C, Bradford SA, Li T, Li B, Huang Y. Can nanoscale surface charge heterogeneity really explain colloid detachment from primary minima upon reduction of solution ionic strength? *J Nanopart Res* 2018;20:165. DOI

71.   Krasowska M, Zawala J, Malysa K. Air at hydrophobic surfaces and kinetics of three phase contact formation. *Adv Colloid Interface Sci* 2009;147-8:155-69. DOI PubMed

72.   Koh P, Schwarz M. CFD modelling of bubble-particle attachments in flotation cells. *Miner Eng* 2006;19:619-26. DOI

73.   Calgaroto S, Azevedo A, Rubio J. Flotation of quartz particles assisted by nanobubbles. *Int J Miner Process* 2015;137:64-70. DOI

74.   Zhang X, Manica R, Tang Y, Tchoukov P, Liu Q, Xu Z. Probing boundary conditions at hydrophobic solid-water interfaces by dynamic film drainage measurement. *Langmuir* 2018;34:12025-35. DOI PubMed

75.   Liu S, Xie L, Liu G, Zhong H, Wang Y, Zeng H. Hetero-difunctional reagent with superior flotation performance to chalcopyrite and the associated surface interaction mechanism. *Langmuir* 2019;35:4353-63. DOI

76.   Contreras-Naranjo JC, Ugaz VM. A nanometre-scale resolution interference-based probe of interfacial phenomena between

microscopic objects and surfaces. *Nat Commun* 2013;4:1919. DOI PubMed PMC

77. Kor M, Korczyk PM, Addai-Mensah J, Krasowska M, Beattie DA. Carboxymethylcellulose adsorption on molybdenite: the effect of electrolyte composition on adsorption, bubble-surface collisions, and flotation. *Langmuir* 2014;30:11975-84. DOI PubMed

78. Filippov L, Javor Z, Piriou P, Filippova I. Salt effect on gas dispersion in flotation column - bubble size as a function of turbulent intensity. *Miner Eng* 2018;127:6-14. DOI

79. Tabor RF, Chan DYC, Grieser F, Dagastine RR. Anomalous stability of carbon dioxide in pH-controlled bubble coalescence. *Angew Chem Int Ed Engl* 2011;50:3454-6. DOI PubMed

80. Cui X, Shi C, Zhang S, et al. Probing the effect of salinity and ph on surface interactions between air bubbles and hydrophobic solids: implications for colloidal assembly at air/water interfaces. *Chem Asian J* 2017;12:1568-77. DOI PubMed

81. Vakarelski IU, Manica R, Tang X, et al. Dynamic interactions between microbubbles in water. *Proc Natl Acad Sci U S A* 2010;107:11177-82. DOI PubMed PMC

82. Kirkpatrick R, Lockett M. The influence of approach velocity on bubble coalescence. *Chem Eng Sci* 1974;29:2363-73. DOI

83. Yang W, Luo Z, Lai Q, Zou Z. Study on bubble coalescence and bouncing behaviors upon off-center collision in quiescent water. *Exp Therm Fluid Sci* 2019;104:199-208. DOI

84. Zhang L, Shi C, Lu Q, Liu Q, Zeng H. Probing molecular interactions of asphaltenes in heptol using a surface forces apparatus: implications on stability of water-in-oil emulsions. *Langmuir* 2016;32:4886-95. DOI

85. Vakarelski IU, Yang F, Thoroddsen ST. Free-rising bubbles bounce more strongly from mobile than from immobile water-air interfaces. *Langmuir* 2020;36:5908-18. DOI PubMed PMC

86. Vakarelski IU, Yang F, Tian YS, Li EQ, Chan DYC, Thoroddsen ST. Mobile-surface bubbles and droplets coalesce faster but bounce stronger. *Sci Adv* 2019;5:eaaw4292. DOI PubMed PMC